Honeycomb Carbon: A Review of Graphene

Matthew J. Allen,[†] Vincent C. Tung,[‡] and Richard B. Kaner*[,†,‡]

Department of Chemistry and Biochemistry and California NanoSystems Institute, and Department of Materials Science and Engineering, University of California, Los Angeles, Los Angeles, California 90095

Received February 20, 2009

Contents

1. Introduction

Graphene is the name given to a two-dimensional sheet of sp^2-hybridized carbon. Its extended honeycomb network is the basic building block of other important allotropes; it can be stacked to form 3D graphite, rolled to form 1D nanotubes, and wrapped to form 0D fullerenes. Long-range π-conjugation in graphene yields extraordinary thermal, mechanical, and electrical properties, which have long been the interest of many theoretical studies and more recently became an exciting area for experimentalists.

While studies of graphite have included those utilizing fewer and fewer layers for some time,[1] the field was delivered a jolt in 2004, when Geim and co-workers at Manchester University first isolated single-layer samples from graphite (see Figure 1).[2] This led to an explosion of interest, in part because two-dimensional crystals were thought to be thermodynamically unstable at finite temperatures.[3,4] Quasi-two-dimensional films grown by molecular beam epitaxy (MBE) are stabilized by a supporting substrate, which often plays a significant role in growth and has an appreciable influence on electrical properties.[5] In contrast, the mechanical exfoliation technique used by the Manchester group isolated the two-dimensional crystals from three-dimensional graphite. Resulting single- and few-layer flakes were pinned to the substrate by only van der Waals forces and could be made free-standing by etching away the substrate.[6−9] This minimized any induced effects and allowed scientists to probe graphene's intrinsic properties.

The experimental isolation of single-layer graphene first and foremost yielded access to a large amount of interesting physics.[10,11] Initial studies included observations of graphene's ambipolar field effect,[2] the quantum Hall effect at room temperature,[12−17] measurements of extremely high carrier mobility,[7,18−20] and even the first ever detection of single molecule adsorption events.[21,22] These properties generated huge interest in the possible implementation of graphene in a myriad of devices. These include future generations of high-speed and radio frequency logic devices, thermally and electrically conductive reinforced composites, sensors, and transparent electrodes for displays and solar cells.

Despite intense interest and continuing experimental success by device physicists, widespread implementation of graphene has yet to occur. This is primarily due to the difficulty of reliably producing high quality samples, especially in any scalable fashion.[23] The challenge is really 2-fold because performance depends on both the number of layers present and the overall quality of the crystal lattice.[19,24−26] So far, the original top-down approach of mechanical exfoliation has produced the highest quality samples, but the method is neither high throughput nor high-yield. In order to exfoliate a single sheet, van der Waals attraction between exactly the first and second layers must be overcome without disturbing any subsequent sheets. Therefore, a number of alternative approaches to obtaining single layers have been explored, a few of which have led to promising proof-of-concept devices.

Alternatives to mechanical exfoliation include primarily three general approaches: chemical efforts to exfoliate and stabilize individual sheets in solution,[27−32] bottom-up methods to grow graphene directly from organic precursors,[33−36] and attempts to catalyze growth *in situ* on a substrate.[37−43] Each of these approaches has its drawbacks. For chemically derived graphene, complete exfoliation in solution so far requires extensive modification of the 2D crystal lattice, which degrades device performance.[31,44] Alternatively, bottom-up techniques have yet to produce large and uniform

[†] Department of Chemistry and Biochemistry and California NanoSystems Institute.
[‡] Department of Materials Science and Engineering and California NanoSystems Institute.

10.1021/cr900070d
Published on Web 07/17/2009

Matthew J. Allen is a graduate student in the Kaner laboratory at the University of California, Los Angeles (UCLA). He received his B.S. in physics at Rice University, where he researched carbon nanostructures in the laboratories of Richard Smalley and Robert Curl.

Vincent C. Tung is a graduate student in the Yang laboratory coadvised by Prof. Kaner at the University of California, Los Angeles (UCLA). He received his M.S. in chemistry from the National Tsing-Hua University in Hsinchu, Taiwan. His previous work was on the photochemistry of organic light emitting diodes (OLEDs).

single layers. Total organic syntheses have been size limited because macromolecules become insoluble and the occurrence of side reactions increases with molecular weight.[36] Substrate-based growth of single layers by chemical vapor deposition (CVD) or the reduction of silicon carbide relies on the ability to walk a narrow thermodynamic tightrope.[40] After nucleating a sheet, conditions must be carefully controlled to promote crystal growth without seeding additional second layers or forming grain boundaries.

Despite tremendous progress with alternatives, mechanical exfoliation with cellophane tape still produces the highest quality graphene flakes available. This fact should not, however, dampen any interest from chemists. On the contrary, the recent transition from the consideration of graphene as a "physics toy" to its treatment as a large carbon macromolecule offers new promise. Years of carbon nanotube, fullerene, and graphite research have produced a myriad of chemical pathways for modifying sp^2 carbon structures,[45−50] which will undoubtedly be adapted to functionalize both the basal plane of graphene and its reactive edges. This not only promises to deliver handles for exploiting graphene's intrinsic properties but also should to lead to new properties altogether.

This review will discuss the field of graphene from a materials chemistry standpoint. After a brief history of the topic, the exciting progress made since 2004, in both the production of graphene and its implementation in devices,

Richard B. Kaner received a Ph.D. in inorganic chemistry from the University of Pennsylvania in 1984. After carrying out postdoctoral research at the University of California, Berkeley, he joined the University of California, Los Angeles (UCLA), in 1987 as an Assistant Professor. He was promoted to Associate Professor with tenure in 1991 and became a Full Professor in 1993. Professor Kaner has received awards from the Dreyfus, Fulbright, Guggenheim, and Sloan Foundations, as well as the Exxon Fellowship in Solid State Chemistry and the Buck−Whitney Research Award from the American Chemical Society for his work on refractory materials, including new synthetic routes to ceramics, intercalation compounds, superhard materials, graphene, and conducting polymers.

will be discussed. For a thorough discussion focused on the physics of graphene, see refs 10, 11, 51, and 52.

2. Brief History of Graphene

To understand the trajectory of graphene research, it is useful to consider graphene as simply the fewest layer limit of graphite. In this light, the extraordinary properties of honeycomb carbon are not really new. Abundant and naturally occurring, graphite has been known as a mineral for nearly 500 years. Even in the middle ages, the layered morphology and weak dispersion forces between adjacent sheets were utilized to make marking instruments, much in the same way that we use graphite in pencils today. More recently, these same properties have made graphite an ideal material for use as a dry lubricant, along with the similarly structured but more expensive compounds hexagonal boron

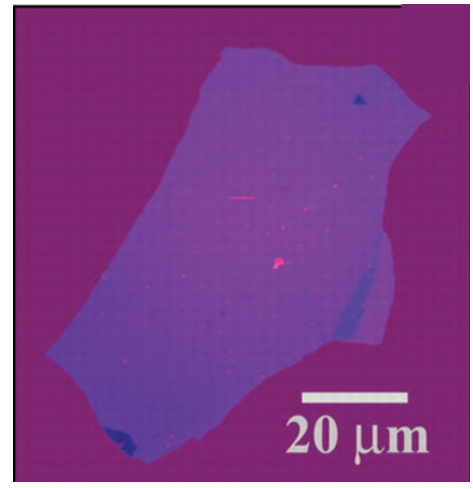

Figure 1. Single layer graphene was first observed by Geim and others at Manchester University. Here a few layer flake is shown, with optical contrast enhanced by an interference effect at a carefully chosen thickness of oxide. (Reprinted with permission from *Science* (http://www.aaas.org), ref 2. Copyright 2006 American Association for the Advancement of Science.)

nitride and molybdenum disulfide. High, in-plane electrical ($\sim 10^4\ \Omega^{-1}\ cm^{-1}$) and thermal conductivity ($\sim$3000 W/mK) enable graphite to be used in electrodes and as heating elements for industrial blast furnaces.[53,54] High mechanical stiffness of the hexagonal network (1060 GPa) is also utilized in carbon fiber reinforced composites. These uses and others generate an annual demand of more than 1 million tons of graphite worldwide.[55]

The anisotropy of graphite's material properties continues to fascinate both scientists and technologists. The s, p_x, and p_y atomic orbitals on each carbon hybridize to form strong covalent sp^2 bonds, giving rise to 120 ° C−C−C bond angles and the familiar chicken-wire-like layers. The remaining p_z orbital on each carbon overlaps with its three neighboring carbons to form a band of filled π orbitals, known as the valence band, and a band of empty π^* orbitals, called the conduction band. While three of the four valence electrons on each carbon form the σ (single) bonds, the fourth electron forms one-third of a π bond with each of its neighbors producing a carbon−carbon bond order in graphite of one and one-third. With no chemical bonding in the *c*-direction, out-of-plane interactions are extremely weak. This includes the propagation of charge and thermal carriers, which leads to out-of-plane electrical and thermal conductivities that are both more than 10^3 times lower than those of their in-plane analogues.[56]

2.1. Chemistry of Graphite

Graphite has a rich chemistry in which it can participate in reactions as either a reducing agent (electron donor) or an oxidizer (electron acceptor). This is a direct consequence of its electronic structure, which results in both an electron affinity and an ionization potential of 4.6 eV.[53]

A large number of experiments for graphite focus on the insertion of additional chemical species between the basal planes, or intercalation. Shaffault is credited with the first intercalation compound using potassium, dating back to 1841.[57] Graphite intercalation compounds (GICs) appear to be the only layered compounds sufficiently ordered to exhibit "staging" in which the number of graphitic layers in between adjacent intercalants can be varied in a controlled fashion. The stage of a compound refers to the number of graphitic layers in between adjacent planes of intercalant. The interlayer spacing can increase from 0.34 nm (3.4 Å) in native graphite to more than 1 nm in some GICs, which further exaggerates the anisotropy of many properties.[56,58]

The increased interlayer spacing in GICs also means a significant reduction in the van der Waals forces between adjacent sheets, which leads one to consider their exfoliation as a possible route to single layers of graphene. Our group tried just that in 2003 by violently reacting a stage-1 potassium intercalation compound (KC_8) with various solvents such as alcohols, but exfoliation produced only metastable slabs around 30 layers thick that had a tendency to scroll under high-powered sonication (see Figure 2).[53,59,60] The interlayer spacing in GICs can be further increased by thermal shock to produce "expanded" graphite, which has now served as a starting material for recent techniques, including a nanoribbon synthesis developed by Dai (see Figure 3).[53,61]

A second focus of experiments on graphite has been substitutional doping by the replacement of carbon with other elements. This includes work by Bartlett and co-workers at Berkeley in which substitution of carbon with boron and nitrogen resulted in p- and n-type graphite, respectively.[62,63] In light of recent progress with CVD of single layer graphene, such work will almost certainly be revisited as an alternative to external gating for controlling electronic behavior in graphene-based devices, or perhaps to form graphene-only p-n junctions.

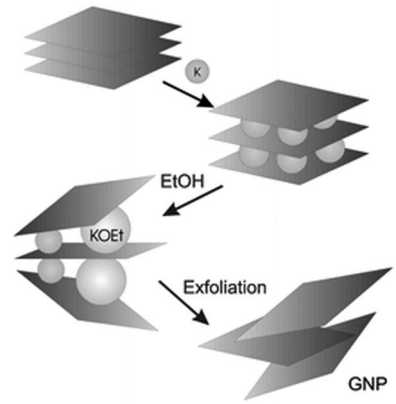

Figure 2. Schematic diagram showing the intercalation and exfoliation process to produce thin slabs of graphite. Potassium is inserted between the layers and reacted violently with alcohols. The exfoliated slabs are $\sim$30 layers thick. (Reprinted with permission by The Royal Society of Chemistry from ref 60.)

It is also important to mention a few points about progress in the chemistry of carbon nanotubes. Among the most important observations have been of the differences in reactivity between the different crystallographic directions (zigzag or armchair).[64−66] This knowledge should transfer directly to the "unrolled" or "flattened" case of planar graphene. A myriad of techniques have also been developed to selectively modify either the sidewalls of carbon nanotubes or their end-caps. Such reactions are important looking forward because they correspond to modification of the basal plane of graphene and its edges. In fact, *in situ* TEM was recently used to study reactions on graphene's zigzag edge by Zettl and others at Berkeley.[67]

3. Down to Single Layers

Researchers have used mechanical exfoliation of layered compounds to produce thin samples for some time. In 1999, Ruoff's group presented one such approach for graphite by using an atomic force microscope (AFM) tip to manipulate small pillars patterned into highly oriented pyrolytic graphite (HOPG) by plasma etching (see Figure 4).[1] The thinnest slabs observed at that time were more than 200 nm thick or the equivalent of $\sim$600 layers. Kim's group at Columbia later improved the method by transferring the pillars to a tipless cantilever, which successively stamped down slabs as thin as 10 nm, or $\sim$30 layers, on SiO_2.[68] Electrical measurements made on the thin crystallites foreshadowed a wealth of work to come. Other early groups working toward graphene included Enoki's in Tokyo, who used temperatures around 1600 °C to convert nanodiamonds into nanometer-sized regions of graphene atop HOPG in 2001.[69]

While these elegant methods produced thin samples, it was ultimately a much simpler approach that led to the first isolation of single layer graphene in 2004 by a Manchester group led by Geim (see Figures 5).[2] In its most basic form, the "peeling" method utilizes common celluphene tape to successively remove layers from a graphite flake. The tape is ultimately pressed down against a substrate to deposit a

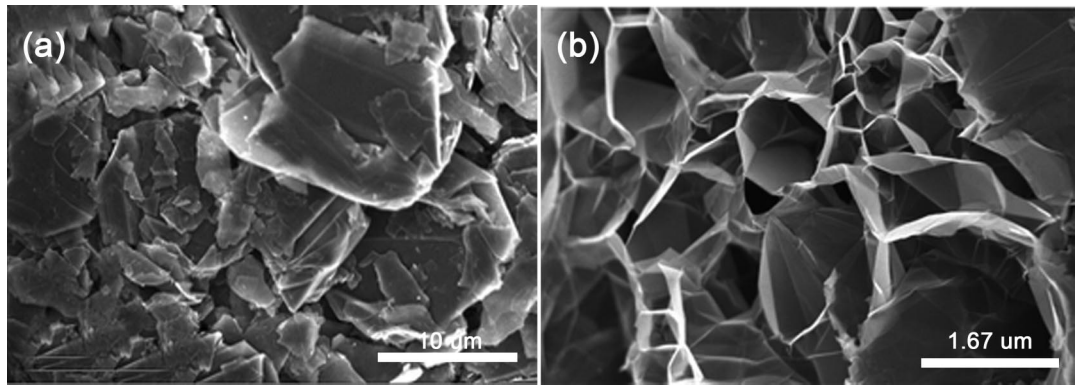

Figure 3. Scanning electron micrographs of natural graphite before (a) and after (b) expansion by acid intercalation and thermal shock. (Reprinted with permission by The Royal Society of Chemistry from ref 60.)

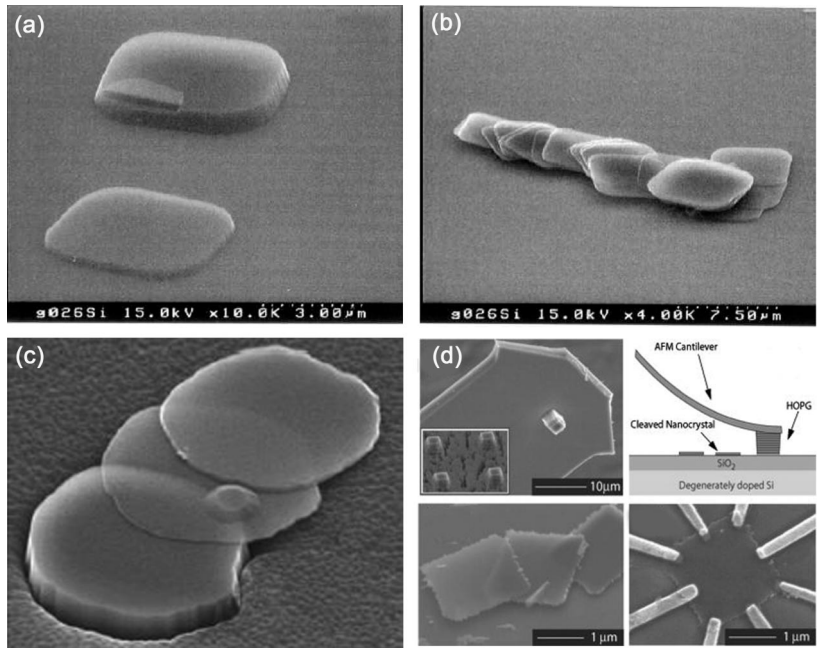

Figure 4. Scanning electron microscope images of early attempts at mechanical exfoliation using graphite pillars. (a and b) Ruoff's group peeled away layers with an AFM tip. (Reprinted with permission from ref 1. Copyright 1999 Institute of Physics.) (c and d) Kim's group transferred the pillars to a tipless cantilever and deposited thin slabs onto other substrates in tapping mode. A series of scanning electron microscope images show thin samples cleaved onto the Si/SiO_2 substrate and a typical mesoscopic device. (Reprinted with permission from ref 68. Copyright 2005 American Institute of Physics.)

sample (see Figure 1). Although the flakes present on the tape are much thicker than one layer, van der Waals attraction to the substrate can delaminate a single sheet when the tape is then lifted away. The method requires a great deal of patience, as depositions put down by inexperienced scientists are often a mess of thick slabs in which locating a single layer can be extremely difficult. With practice, the technique results in high-quality crystallites, which can be more than 100 μm^2 in size.

Perhaps the most important part of isolating single layer graphene for the first time was the ability to spot an atomically thin specimen in some readily identifiable fashion. Optical absorbance of graphene has since been measured at just 2.3%, ruling out direct visual observation (see Figure 6).[70,71] In order to visualize single flakes, the Manchester group took advantage of an interference effect at a specially chosen thickness (300 nm) of SiO_2 on Si to enhance the optical contrast under white-light illumination.[72] Although seemingly a simple idea, this was a major step forward and has contributed a great deal toward progress in this field.

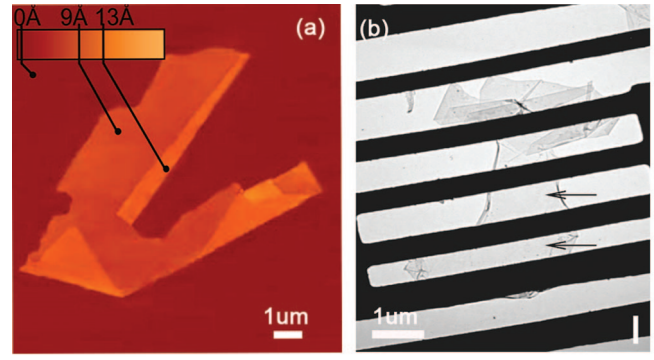

Figure 5. Mechanical exfoliation produced the very first single layer graphene flakes. (a) An atomic force microscopy image shows the substrate−graphene step height of <1 nm and a folded step height of 0.4 nm. (Reprinted with permission from ref 9. Copyright 2005 PNAS.) (b) TEM image of a free-standing graphene film after etching of the underlying substrate. [Reprinted with permission from *Nature* (http://www.nature.com), ref 6. Copyright 2007 Nature Publishing Group.]

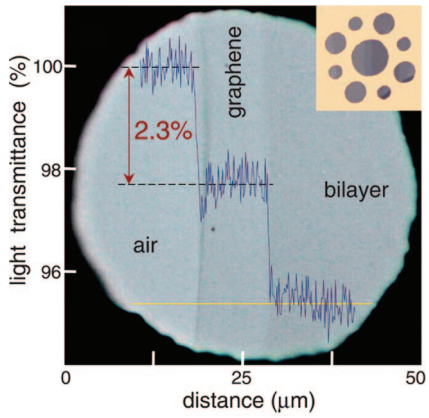

Figure 6. A single and bilayer sample suspended on a porous membrane. Optical absorbance is measured at 2.3% per layer. The inset shows the sample design with several apertures. [Reprinted with permission from *Science* http://www.aaas.org), ref 70. Copyright 2008 American Association for the Advancement of Science.]

Groups have since adapted the same effect to image graphene on a variety of substrates and under nonwhite-light conditions.[72−75]

3.1. Characterizing Graphene Flakes

With new access to 2D crystallites, experimentalists scrambled to confirm results long predicted by theory. Before they could do so, techniques needed to be developed for the characterization of deposited flakes. While optical microscopy using the interference effect was a good method for identifying thin candidates, it could not provide conclusive evidence that a given flake was single, double, or multilayered. This is an important issue because some of the more interesting properties of graphene are dependent on crystallite thickness. The most obvious example is electronic band structure. Single-layer graphene is a zero band gap semiconductor or semimetal in which the highest occupied molecular orbital (HOMO) touches the lowest unoccupied molecular orbital (LUMO) at a single Dirac point. For thicker flakes, stacking of multiple layers leads to some overlap of their carrier wave functions and the overall behavior becomes metallic. To match observations with theory, reliable identification of the number of layers present in a given sample became imperative.

3.1.1. Scanning Probe Microscopy

Scanning probe microscopy was perhaps the most obvious choice for verification of crystallite thickness. The method is relatively slow, but the 0.34 nm (3.4 Å) step height for each successive layer is well within the detection limits for modern atomic force microscopes (AFMs). Resolving the substrate−graphene height profile proved difficult, however, due to the differences in tip attraction/repulsion between the insulating substrate and semimetallic graphene. This issue was exacerbated under ambient conditions by the preferential adsorption of a thin layer of water on graphene. With such complications, reports of substrate−graphene height profiles by atomic force microscopy have typically ranged from 0.6 to 1.0 nm for single layers.[2]

The folded edges of graphene have often provided a more reliable and accurate measurement of thickness under atomic force microscopy because there is no change in material associated with the location of the step. It was such a fold that allowed the Manchester group to confirm the single-layer step height of ∼0.4 nm in their original report (see Figure 5). Although seemingly unlikely, folds commonly occur during mechanical exfoliation because van der Waals attraction between a sheet and itself is sizable and doubling over sometimes provides an energetic minimum.

Scanning tunneling microscopy (STM) has long been used to observe the electronic topography of graphite.[76−78] In these experiments, only three carbons of the six-member rings are visible due to the AB stacking of graphite (see Figure 7).[79] In this arrangement, electron density is considerably higher for the three α-carbons (those that eclipse carbons in the sheet just below), and hence, they are the only ones visible by STM. This is as opposed to what was expected for single layer graphene, in which the six carbons are completely equivalent and thus should all appear with equal intensity. This was indeed confirmed by ultrahigh vacuum STM images taken at Columbia by Flynn and others.[79] Their measurements also gave evidence of the high crystal quality in mechanically exfoliated samples, which showed few-to-no defects over tens of nanometers.

3.1.2. Raman Spectroscopy

While graphene's layered structure makes it ideally suited for further study by scanning probe microscopy, sample preparation time and substrate requirements mean that additional methods are necessary to reliably confirm specimen thickness in a high-throughput fashion. Ultimately it was not a directly topographical technique but instead Raman spectroscopy that emerged as the most useful way to probe the thickness of mechanically exfoliated flakes. Although less than obvious, this makes good sense because the features of graphite and graphene directly reflect changes in electronic structure from the stacking of successive layers.[80−86] Observations of gradual changes in the Raman spectrum allow one to infer the number of layers (up to the screening length) in a "fingerprint" fashion (see Figure 8).

The major features of the Raman spectra of graphite and graphene are the G band at ∼1584 cm^{-1} and the G′ band at ∼2700 cm^{-1}. The G band is due to the E_{2g} vibrational mode, and the G′ band is a second-order two-phonon mode. A third feature, the D band at ∼1350 cm^{-1}, is not Raman active for pristine graphene but can be observed where symmetry is broken by edges or in samples with a high density of defects. It is changes in the positions and relative peak heights of the G and G′ bands that serve to indicate the number of layers present for a given flake. The location of the G peak for single layer graphene is 3−5 cm^{-1} higher than that for bulk graphite, while its intensity is roughly the same. The G′ peak shows a significant change in both shape and intensity as the number of layers is decreased. In bulk graphite, the G′ band is comprised of two components, the intensities of which are roughly $^1/_4$ and $^1/_2$ that of the G peak for the low and high shifts, respectively. For single layer graphene, the G′ band is a single sharp peak at the lower shift, with intensity roughly 4 times that of the G peak. It was fitting to these trends that finally enabled scientists to reliably confirm the identity of mechanically exfoliated flakes.

4. Extraordinary Devices with Peeled Graphene

Mechanical exfoliation and the Raman fingerprinting technique allowed scientists to forge ahead with a full suite

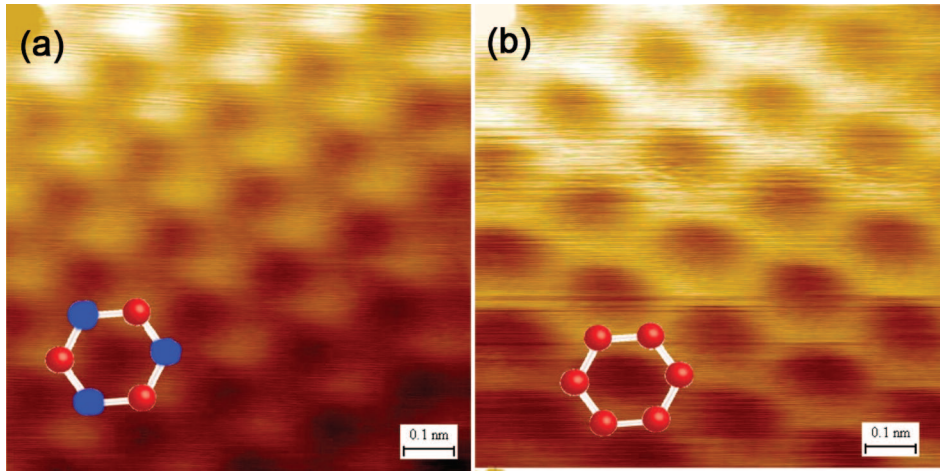

Figure 7. (a) STM image of graphite showing only the three carbons that eclipse a neighbor in the sheet directly below. (b) In contrast, all six carbons are equivalent and thus visible in mechanically exfoliated single-layer graphene. (Reprinted with permission from ref 79. Copyright 2007 PNAS.)

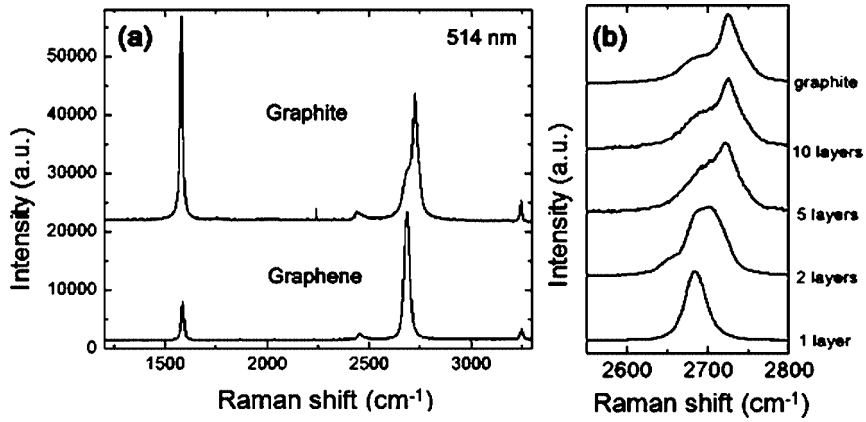

Figure 8. Raman spectroscopy is a powerful diagnostic tool for the study of graphene. Both the G (near 1584 cm^{-1}) and G′ (near 2700 cm^{-1}) bands undergo significant changes due to the thickness of AB stacked flakes, as produced by mechanical exfoliation. (Reprinted with permission from ref 80. Copyright 2006 American Physical Society.)

of experiments on single-layer graphene. These led to a number of extraordinary proof-of-concept devices.

4.1. High-Speed Electronics

Theoretical predictions long suggested extremely high carrier mobility and an ambipolar field-effect in graphene.[87,88] This motivated the very first experiments that wired-up mechanically exfoliated flakes by e-beam lithography.[2,18] Beyond confirming a number of predictions, those measurements generated significant interest in graphene as a possible material for the next generation of semiconductor devices. That attention may or may not be warranted, but many agree that our ability to sustain Moore's law will ultimately become a question of carrier mobility.

Extraordinary electronic properties in graphene are really due to the high quality of its 2D crystal lattice.[9,19,89−91] That high quality implies an unusually low density of defects, which typically serve as the scattering centers that inhibit charge transport. In 2008, Kim's group at Columbia measured a carrier mobility in excess of 200,000 $cm^2/(V\ s)$ for a single layer of mechanically exfoliated graphene (see Figure 9).[7] In their experiments, substrate-induced scattering was minimized by cleverly etching under the channel to produce graphene completely suspended between gold contacts. At such high carrier mobility, charge transport is essentially ballistic on the micrometer-scale at room temperature. This

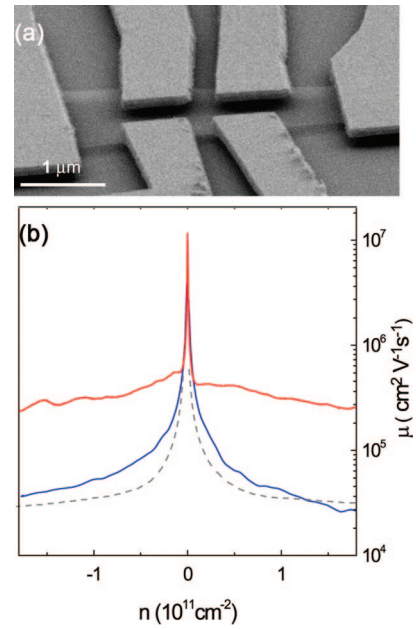

Figure 9. Suspended graphene shows extremely high mobility due to the minimization of substrate-induced scattering. (a) SEM image of a suspended sheet after etching. (b) Field-effect measurements indicate mobility greater than 200,000 $cm^2/(V\ s)$. (Reprinted with permission from ref 7. Copyright 2008 Elsevier.)

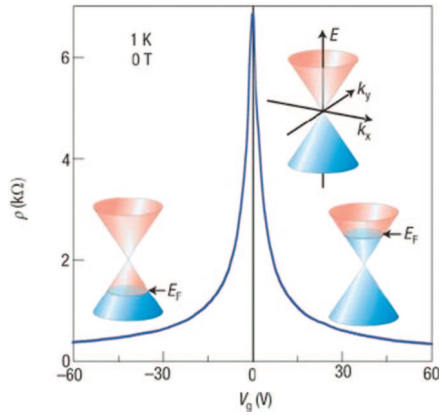

Figure 10. Schematic diagram showing the band structure and resulting ambipolar field effect in graphene. Conduction and valence bands meet at the Dirac point without an external field. Under gate bias, the Fermi level moves above or below the Dirac point to introduce a significant number of free carriers. [Reprinted with permission from *Nature* (http://www.nature.com), ref 10. Copyright 2007 Nature Publishing Group.]

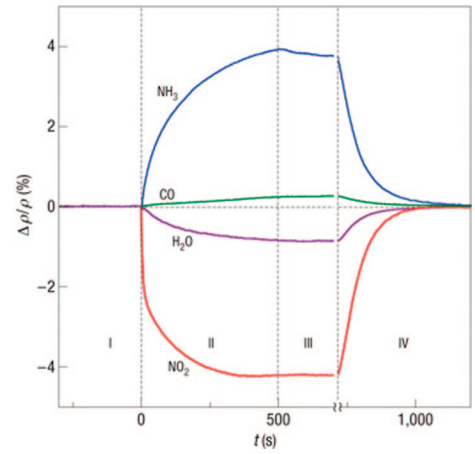

Figure 11. The lack of surface states in graphene makes possible the detection of even single adsorbate. The direction of change in the figure indicates the sign of induced carriers (holes for H_2O and NO_2; electrons for CO and NH_3). [Reprinted with permission from *Nature* (http://www.nature.com), ref 21. Copyright 2007 Nature Publishing Group.]

has major implications for the semiconductor industry because it enables, in principle, fabrication of all-ballistic devices even at today's integrated circuit (IC) channel lengths (currently down to 45 nm).

The second important point about charge transport in graphene is ambipolarity. In the field-effect configuration, this implies that carriers can be tuned continuously between holes and electrons by supplying the requisite gate bias. This can be easily visualized given the unique band structure of graphene (see Figure 10).[10] Under negative gate bias, the Fermi level drops below the Dirac point, introducing a significant population of holes into the valence band. Under positive gate bias, the Fermi level rises above the Dirac point, promoting a significant population of electrons into the conduction band.

Besides motivating academic interest, access to a truly ambipolar semiconductor enables a number of novel device structures. These are fundamentally different from silicon-based logic because doping levels can be dynamically controlled entirely by gating. Momentarily providing local gate biases to different parts of the same flake can form junctions or even more complicated logic. Subsequently rearranging the biases can then completely redefine the device without making any physical changes to the channel material.

4.2. Single Molecule Detection

The second exciting proof-of-concept implementation of mechanically exfoliated graphene was in chemical sensors. Several important features of graphene made it an excellent candidate for the sensing active area. First and foremost, the 2D structure of graphene constitutes an absolute maximum of the surface area to volume ratio in a layered material, which is essential for high sensitivity. In fact, this has been the major motivation behind implementation of other nanostructured materials in sensors. In the case of traditional materials, bulk properties such as resistivity are not substantially influenced by single adsorption events on their surface. In graphene, however, there is no such distinction between surface sites and the bulk material, so every adsorption event is significant.

Versatility of graphene as the basis of a sensor results from its unique electronic structure. The ambipolarity means that adsorption of either electron withdrawing or donating groups can lead to "chemical gating" of the material, which can be easily monitored in a resistive-type sensor setup.

In 2007, single molecule sensitivity to NO_2 and NH_3 was demonstrated by the Manchester group for the first graphene-based sensor (see Figure 11).[21,22] In the case of either analyte, adsorption events induced some population of free carriers and the resistivity of a single layer flake decreased upon exposure. A Hall-type configuration confirmed the opposite sign of carriers generated by the two gases, with an electron-withdrawing species (e.g., NO_2) inducing conduction by holes (p-type) and an electron-donor (e.g., NH_3) inducing conduction by electrons (n-type).

With such exciting early results, experiments with graphene-based sensors have certainly just begun. While there are few questions about the limits of sensitivity for these devices, the real drawback thus far is a lack of selectivity. A sensor is rather impractical if it responds in a similar way upon exposure to any analyte. This is an excellent area of opportunity for chemists. Modification of the basal plane or its edges could certainly incorporate analyte-specific lock-and-key type binding sites. Such an approach would not only provide selective sensitivity to a large variety of chemical species but perhaps also enable detection of biological agents as well. Similar schemes have been successfully demonstrated with carbon nanotubes and quantum wires.[92−95]

5. Alternatives to Mechanical Exfoliation

Exciting progress in the field of graphene, and especially so soon after its initial discovery, began to suggest a bright future. The limiting step for most experiments was simply obtaining good single layers by mechanical exfoliation. This would have greater implications for real-world devices because the process is low throughput and unlikely to be industrially scalable. With this in mind, the challenge of finding an alternate route to single-layer graphene became the focus of a great deal of research.

One should keep in mind three important factors beyond scalability when considering the proficiency of any synthetic route to graphene. First and foremost, a process must produce high quality in the 2D crystal lattice to ensure high mobility. Second, the method must provide fine control over crystallite

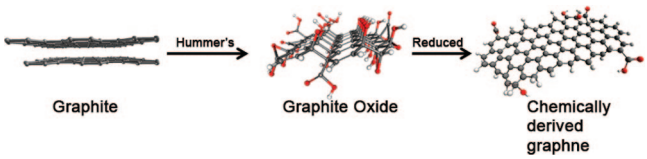

Figure 12. Molecular models show the conversion process from graphite to chemically derived graphene. (Reprinted with permission from ref 101. Copyright 2009 Nature Publishing Group.)

thickness so as to deliver uniform device performance. Finally, and for ease of integration, any process should be compatible with current CMOS (complementary metal-oxide-semiconductor) processing.

5.1. Chemically Derived Graphene from Graphite Oxide

In 2006, Ruoff's group was the first to demonstrate a solution-based process for producing single-layer graphene (see Figure 12).[27,29,96,97] The method hinged on chemical modification of graphite to produce a water dispersible intermediary, graphite oxide (GO). After oxidation by Hummers' method, GO is a layered stack of puckered sheets with AB stacking, which completely exfoliates upon the addition of mechanical energy.[98,99] This is due to the strength of interactions between water and the oxygen-containing (epoxide and hydroxyl) functionalities introduced into the basal plane during oxidation. The hydrophilicity leads water to readily intercalate between the sheets and disperse them as individuals.

Although GO itself is nonconducting, the graphitic network can be substantially restored by thermal annealing or through treatment with chemical reducing agents, a number of which have been explored. Ruoff's group detailed the use of hydrazine hydrate to eliminate oxidation through the formation and removal of epoxide complexes.[29] This was done by adding hydrazine directly to aqueous dispersions of GO. In their original report, the reduced single sheets were used as an additive for polystyrene-based composites.[27,100] The 2D geometry led to an extremely low percolation threshold of just 0.1%, enhancing both the conductivity and strength of the matrix.

One problem with the original aqueous reduction of GO was that the removal of oxygen groups caused the reduced sheets to become less hydrophilic and quickly aggregate in solution. Gordon Wallace, Dan Li, and co-workers in collaboration with our group later showed that raising the pH during reduction leads to charge-stabilized colloidal dispersions, even of the deoxygenated sheets.[30] Recently we've improved the reduction step by making dispersions directly in anhydrous hydrazine.[101−103] Note that use of hydrazine requires great care because it is both highly toxic and potentially explosive.[104]

The most exciting advantages of the GO method are its low-cost and massive scalability. The starting material is simple graphite, and the technique can easily be scaled-up to produce gram quantities or larger of "chemically derived graphene" dispersed in a liquid. GO is also an interesting material in its own right for composites applications. Ruoff's group has demonstrated free-standing films with extremely high tensile strength up to ∼42 GPa (see Figure 13).[105,106]

5.1.1. Depositions

Obtaining uniform and reproducible depositions is one for the most important requirements for incorporating a solution-based technique into device fabrication. Furthermore, the type of deposition required can range widely depending on the design specifics of a given device. Well-suited to this task, chemically converted graphene suspensions are versatile and have permitted a large number of deposition techniques (see Figure 14).[101,107−109] These have been used to produce films with coverage ranging anywhere from evenly spaced single sheets to densely packed overlapping films.

The original technique used by our group for depositing films was spray coating from water onto a heated substrate.[31] Although we were able to isolate and characterize some single sheets, high surface tension caused significant aggregation even if the substrate was heated to flash-dry the suspension upon contact. We have been more successful spin-coating dispersions made directly in hydrazine. The method allows for a full range of coverage densities by fine-tuning of spin-speed and a pretreatment applied to the surface of the substrate.

Huang's group at Northwestern recently demonstrated wonderful control over depositions using Langmuir−Blodgett assembly of GO.[107] They showed that electrostatic repulsion prevents the single layers from overlapping when compressed at an air/surface interface. This led to depositions on SiO_2 that included dilute, close-packed, and overpacked films. Dai's group at Stanford has done similar work with Langmuir−Blodgett techniques and also layer-by-layer assembly using electrostatic attraction to biased substrates.[109]

5.1.2. Defect Density in Chemically Derived Graphene

As with mechanically exfoliated graphene, it is important to characterize chemically derived flakes before fabricating devices. This is especially true in the chemical case because the basal plane of graphene undergoes serious alteration during the process of oxidation and reduction. Residual oxidation was made obvious by an appreciable D band near 1350 cm^{-1} in the Raman spectrum of chemically derived graphene.[29] This band is made Raman active by the significant number of defects and resulting broken symmetry of the basal plane. X-ray photoelectron spectroscopy (XPS) of reduced GO indicates nearly complete removal of oxygen, which has led Ruoff's group and our own to surmise that nonconjugated sp^3 carbon constitutes most of the defects. These also limit the observation of interesting physics phenomena in chemically derived graphene and inhibit mobility.

The presence of a large D band also precludes the fingerprinting technique that is used to determine crystallite thickness for mechanically exfoliated graphene. The prominence of the band makes assigning any exact position to the G band next to impossible. Instead, most groups have turned to atomic force microscopy in order to confirm the thickness of deposited flakes. As in other cases, the graphene-substrate step height is difficult to resolve and reports range between 0.4 and 1.0 nm for single layers.[30,101,107]

5.1.3. Field-Effect Devices

Even at a lower overall crystal quality, the availability of chemically derived graphene has removed a serious logjam in the engineering of graphene-based devices and scientists have been eager to make electrical measurements. The first

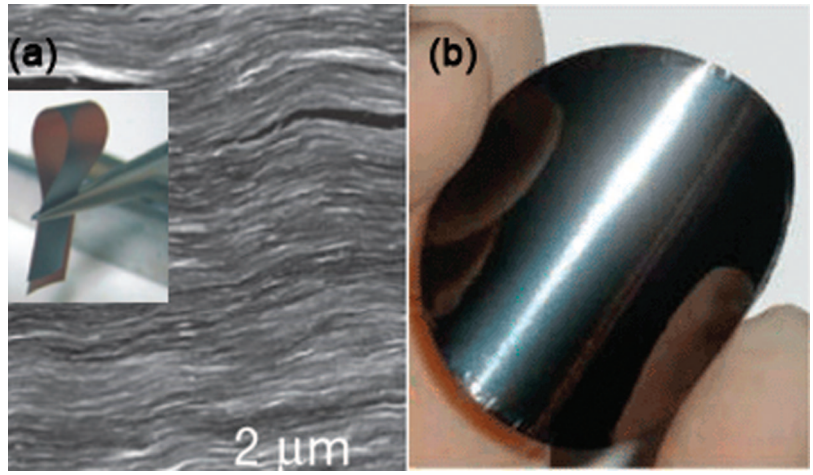

Figure 13. Free-standing graphene films show extremely high tensile strength. (a) Cross-sectional SEM image of graphite oxide stacking in a film produced by filtration. [Reprinted with permission from *Nature* (http://www.nature.com), ref 105. Copyright 2007 Nature Publishing Group.] (b) Chemical reduction produces a film with shiny luster [Reprinted with permission from *Science* (http://www.aaas.org), ref 125. Copyright 2008 American Association for the Advancement of Science.]

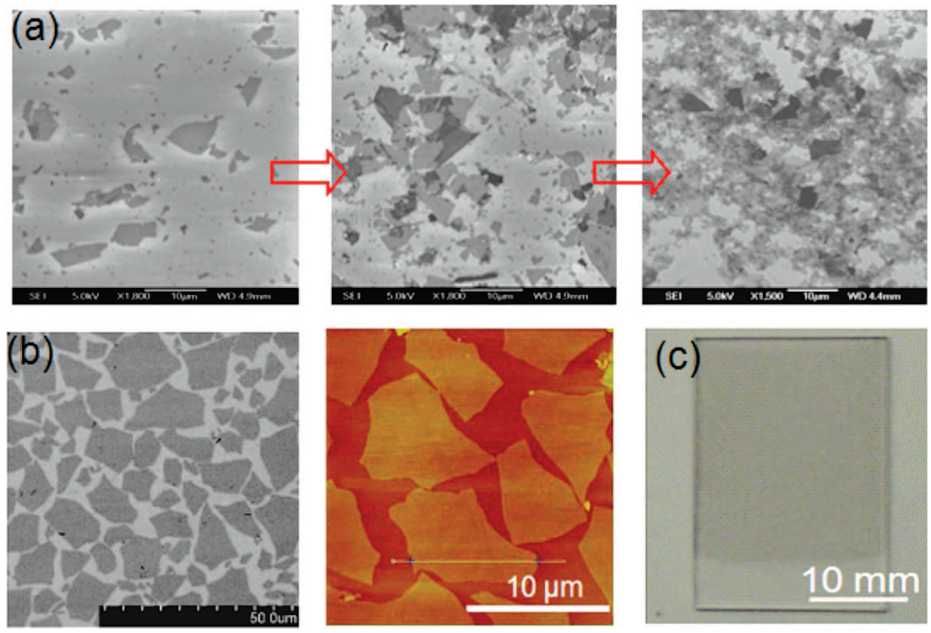

Figure 14. Solution processing allows deposition of synthesized/modified graphene in a variety of densities. (a) SEM images of different films spin-coated from hydrazine. (b) SEM and atomic force microscopy images of a graphite oxide film deposited by Langmuir−Blodgett assembly. (Reprinted with permission from ref 107. Copyright 2009 American Chemical Society.) (c) Multilayer coatings are still quite transparent. [Reprinted with permission from *Nature* (http://www.nature.com), ref 109. Copyright 2008 Nature Publishing Group.]

devices were fabricated by e-beam lithography on flakes around 1 μm^2 in size.[31] More recently, Ruoff's group and our own have produced much larger flakes, which enabled us to demonstrate scalable arrays of field-effect devices using conventional photolithography (see Figure 15).[96,101]

The quality of the 2D lattice in chemically derived graphene is sacrificed during oxidation as the hybridization of many carbons changes from planar sp^2 to tetrahedral sp^3 and the sheet puckers. This has several consequences in device performance. Unlike those made from mechanically derived graphene, we observed p-type current modulation for top-contact and back-gated field-effect devices. We attribute this to residual oxidation, which provides deep trap states for electrons and limits any gate modulation to that of holes. Another consequence is inhibited mobility, which we estimate at less than 1000 $cm^2/(V\ s)$.

While these properties have led some to question the appropriateness of chemically derived graphene-based devices, the material has provided an excellent platform for testing novel device structures. Furthermore, researchers have gained valuable experience integrating a solution-based technique into device fabrication. Those methods will carry over should a less-severe route to complete exfoliation be developed.

5.1.4. Practical Sensors

While single-molecule detection from mechanically exfoliated graphene was an exciting proof-of-principle, the difficulty of producing thin specimens and the requirement of ultrahigh vacuum limits the practicality of these devices. Recently, a number of groups, including Robinson's at the Naval Research Laboratory and our own, have demonstrated good sensitivity for NO_2, NH_3, and dinitrotoluene under ambient conditions using chemically derived graphene (see Figure 16).[103,110]

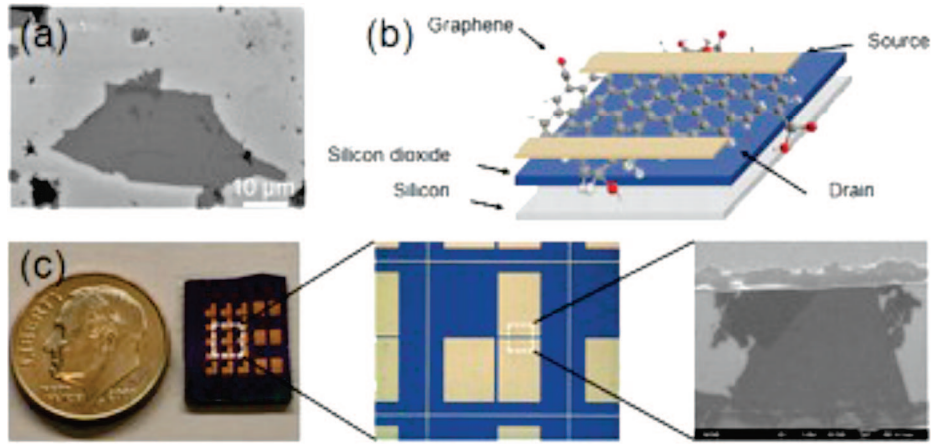

Figure 15. (a) SEM image of a large single sheet deposited on SiO_2. (b) Schematic view of a top-contact, back-gated device. (c) Photograph (left), optical image (middle), and SEM image (right) of a working device with a channel length of 7 μm. (Reprinted with permission from ref 101. Copyright 2009 Nature Publishing Group.)

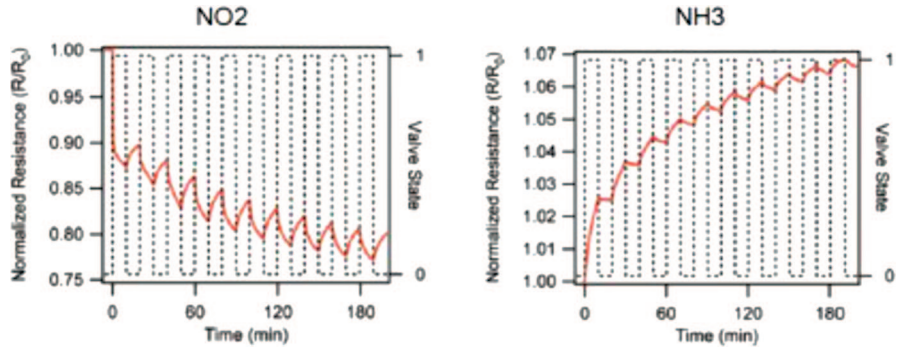

Figure 16. Chemically derived graphene provides a practical route to graphene-based resistive sensors. The resistance of the p-type material decreases upon exposure to electron withdrawers (e.g., NO_2) and increases upon exposure to electron donors (e.g., NH_3). (Reprinted with permission from ref 103. Copyright 2009 American Chemical Society.)

It is interesting to note the differences in response of chemically derived graphene sensors and mechanically exfoliated ones. As discussed earlier, electron donating or withdrawing groups increase electron or hole populations in pristine graphene and thus both lead to increased conductivity. Chemically derived graphene is nominally p-type. Therefore, electron withdrawing groups contribute additional carriers, but electron donators actually serve to deplete holes from the valence band. Hence, NO_2 and NH_3 led to opposite directions of response in our sensors.

5.1.5. Transparent Electrodes

Solution processing of chemically derived graphene and the depositions achieved soon led researchers to consider using the material in transparent conductors. The demand for such coatings has grown rapidly due to optoelectronic devices including displays, LEDs, and solar cells. While the current industry standard is indium tin oxide (ITO), carbon nanotubes have long been touted as a possible alternative due to their low dimensionality and ability to form a percolating conductive network at extremely low densities. The same merits make graphene an obvious choice.

Mullen and co-workers demonstrated the first graphene-based transparent conductor.[111] Films were deposited by dip-coating with GO and reducing by thermal annealing. Sheet resistances as low as 0.9 kΩ/◊ were obtained at 70% transmittance. While the performance was considerably less than that of ITO (70 Ω/◊ at 90% transmittance), the films were low-cost and did not require vacuum sputtering. The group also used the film as the anode in a dye-sensitized solar cell, which had a power conversion efficiency (PCE) of 0.26%. Chhowalla's group later fabricated a polymer solar cell with a PCE of 0.1% using a similar film.[112,113] The performance of these cells was less than that of the corresponding control devices on ITO, but they provide a proof-of-concept for low-cost transparent coatings based on graphene.

5.2. Total Organic Synthesis

Although graphite oxide has produced the first chemically derived micrometer-scale graphene, synthetic techniques for smaller planar, benzene-based macromolecules have been known for some time.[33,34,114−117] These graphene-like polyacyclic hydrocarbons (PAHs) occupy an interesting place in between "molecular" and "macromolecular" structures and are now attracting new interest as a possible alternative route to graphene.

PAHs are attractive because they are highly versatile and can be substituted with a range of aliphatic chains to modify solubility.[36] Thus far, the major drawback of PAHs has been their limited size range. This is due to the fact that increasing molecular weight generally decreases solubility and increases the occurrence of side reactions. Under these conditions, preservation of dispersibility and a planar morphology for large PAHs has been very challenging.

A major advance came in 2008, when Mullen and co-workers reported the synthesis of nanoribbon-like PAHs up to 12 nm in length (see Figure 17).[35] Although the electronic properties of these nanoribbons have yet to be characterized,

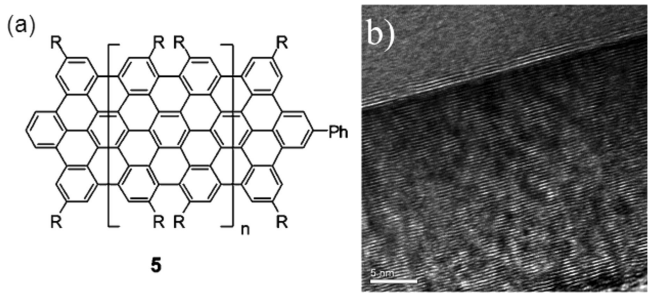

Figure 17. Polyacyclic aromatic hydrocarbons (PAHs) may offer a ground-up synthesis of graphene. (a) Chemical structure of PAHs and (b) TEM of a nanoribbon synthesized by Mullen. (Reprinted with permission from ref 35. Copyright 2008 American Chemical Society.)

they may indeed exhibit graphene-like behavior. If researchers in this area are able to further extend the size range of PAHs in the coming years, this could provide a clean synthetic route to graphene for some applications. In any event, the organic techniques developed will have important implications for modification of or addition to conjugated carbon macromolecules.

5.3. Epitaxial Graphene and Chemical Vapor Deposition

While solution-based synthetic schemes aim to circumvent the need for support substrates, two techniques take advantage of specially chosen platforms to encourage growth of high quality graphene.

De Heer and others at the Georgia Institute of Technology pioneered an epitaxial method in which graphene results from the high temperature reduction of silicon carbide (see Figure 18).[38−40,118−120] The process is relatively straightforward, as silicon desorbs around 1000 °C in ultrahigh vacuum. This leaves behind small islands of graphitized carbon, which were first located by STM and electron diffraction experiments. More recently, groups have used photolithography to pattern epitaxial growth in predetermined locations and to make devices.[119]

A number of physical properties differ between epitaxially grown and mechanically exfoliated graphene.[37,39] This is due to the influence of interfacial effects in epitaxial graphene, which are heavily dependent on both the silicon carbide substrate and several growth parameters. For epitaxial graphene, differences in the periodicity observed by STM and LEEDS are not well understood.[121] The same is true for the energy gap observed by angle-resolved photoemission spectroscopy (ARPES).[122]

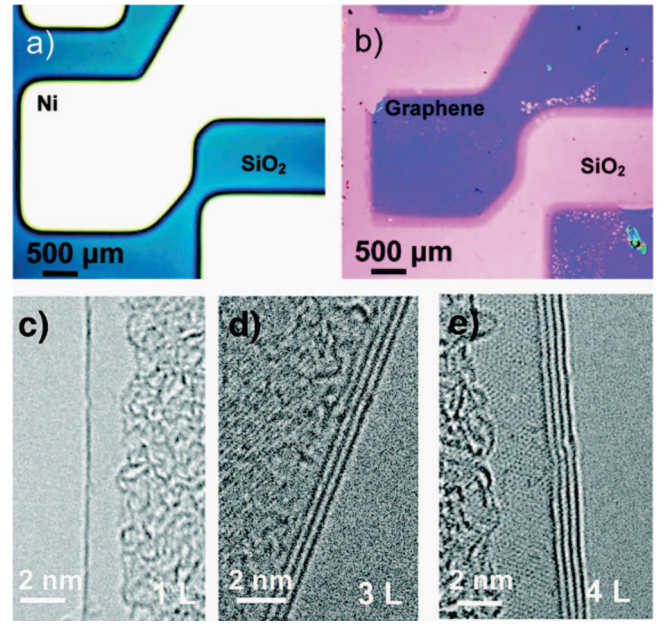

Figure 19. Chemical vapor deposition of graphene on transition metal substrates. Optical microscope image of (a) the nickel catalyst and (b) the resulting graphene film. TEM images show the nucleation of (c) one, (d) three, or (e) four layers during the growth process. (Reprinted with permission from ref 41. Copyright 2009 American Chemical Society.)

The second substrate-based method is chemical vapor deposition (CVD) of graphene on transition metal films (see Figure 19). Groups at MIT and in Korea pioneered the process, which relies on the carbon-saturation of a transition metal upon exposure to a hydrocarbon gas at high temperature.[41−43] Most often, nickel films are used with methane gas. Upon cooling the substrate, the solubility of carbon in the transition metal decreases and a thin film of carbon is thought to precipitate from the surface.

One of the major advantages of substrate-based methods for graphene synthesis is their high compatibility with current CMOS technology. In theory, both epitaxial and CVD techniques have the prospect of producing a single sheet of graphene over an entire wafer, which may be the simplest way to integrate the new material into current semiconductor processes and devices. The remaining challenge for epitaxial and CVD methods is obtaining fine control over film

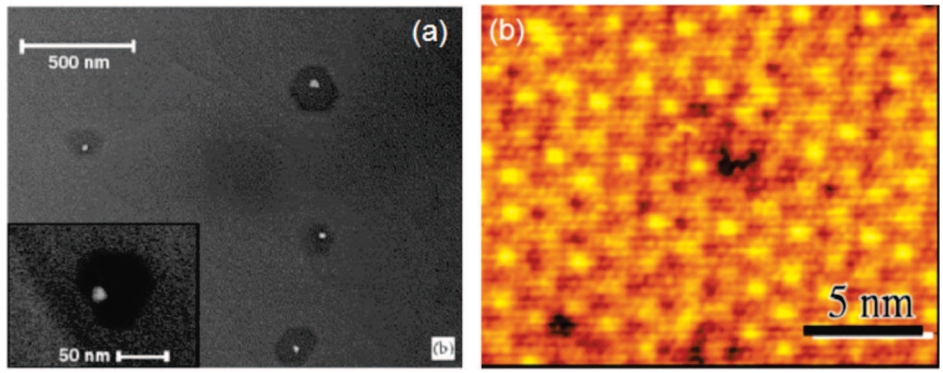

Figure 18. Silicon carbide is reduced to graphene as silicon sublimes at high temperature. (a) SEM image shows small hexagonal crystallites. (Reprinted with permission from ref 120. Copyright 2006 Elsevier.) (b) STM image shows long-range order and a low density of defects. [Reprinted with permission from *Science* (http://www.aaas.org), ref 38. Copyright 2006 American Association for the Advancement of Science.]

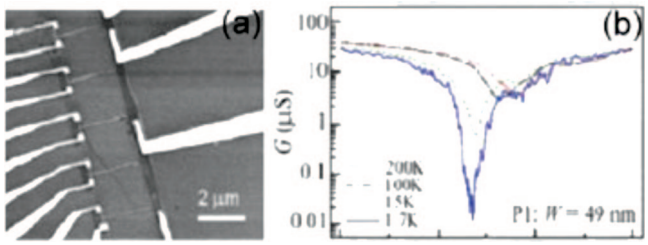

Figure 20. Nanoribbons offer enhanced transistor behavior due to quantum confinement. (a) SEM image of nanoribbons defined by photolithography and O_2 plasma etching. (b) Kim's group demonstrated I_{on}/I_{off} ratios as high as 10^4 at widths of ~50 nm. (Reprinted with permission from ref 124. Copyright 2007 American Physical Society.)

thickness and preventing secondary crystal formation. In an ideal case, both methods rely on the nucleation and growth of a single crystal without the formation of a boundary or seeding of a second layer. Currently, the best specimens have a variation in thickness of perhaps 1−3 layers and are polycrystalline. Field effect devices fabricated with epitaxial and CVD graphene display carrier mobilities in excess of 1000 $cm^2/(V\ s)$.[42,118]

In the case of CVD graphene, etching of the underlying metal allows the carbon films to be transferred to other substrates. This, combined with the large area of depositions, has great promise for transparent conducting applications. One such film grown by CVD and transferred via a PDMS stamp onto glass showed a sheet resistance of just 280 Ω/◊ at 80% optical transmittance.[42]

6. Graphene Nanoribbons

A major issue with graphene-based logic devices is their poor I_{on}/I_{off} ratios. Conductivity in graphene is minimized under zero gate bias, but devices are essentially impossible to turn off at any reasonable temperature because thermal energy and fluctuations are more than sufficient to produce large carrier populations. This high "leakage" current results in I_{on}/I_{off} ratios that are typically just 1 or 2 orders of magnitude, which is insufficient for implementation in real devices.

While a number of approaches have been suggested, the most straightforward way to minimize the off current in graphene-based devices is to introduce an appreciable band gap. This has motivated a great deal of research into graphene nanoribbons, which are no longer semimetallic due to quantum confinement. In 2007, Kim's group used e-beam patterning and oxygen (O_2) plasma etching of mechanically exfoliated graphene to make the first sub-50 nm nanoribbons (see Figure 20).[123,124] Although the process yielded I_{on}/I_{off} ratios of up to 10^4, devices showed high variability due to the lack of control over edge termination. Stencil-like patterning was indiscriminate of crystallographic direction, and thus edge effects were essentially different every time.

The challenge of synthesizing reproducible graphene nanoribbons is an interesting one for chemists, who have sought to exploit the differences in reactivity along graphene's two crystallographic directions.[64] In 2008, Dai's group at Stanford developed the first technique for isolating nanoribbons directly from bulk graphite (See Figure 21).[61] It involved sonication of expanded graphite in the presence of a polymer known to participate in π-stacking with conjugated carbons. The polymer acted to noncovalently functionalize and consequently stabilize nanoribbons formed by mechanical fracture. Atomic force microscopy of the nanoribbons suggests that fracture follows nicely along the crystallographic directions of graphene. In the presence of the polymer, the ribbons can be suspended in organic solvents and then deposited by spin-coating.

Electrical testing of Dai's nanoribbons showed much greater consistency than those made by lithography. As predicted by theory, the band gap (E_g) of nanoribbons was found to be inversely proportional to their width, with an E_g of ~0.4 eV for specimens fewer than 10 nm wide. This led to I_{on}/I_{off} ratios of up to 10^6 for the thinnest strips. The next major challenge will be finding a way to reliably deposit the nanoribbons in predefined locations for scalable device fabrication.

7. Future Work

Graphene has an interesting history, but many now wonder about its future. The subject of considerable scholarly debate, it does seem reasonable to assert a few things looking ahead. First, the quality and availability of "synthetic" graphene will continue to improve. Whether high quality material comes in the form of an alternative chemical route to the complete exfoliation of graphite or from optimization of the thermal processes required for substrate-based methods, there is no sign that synthetic techniques are nearing their upper limit. This means that device engineers will have ample access to improved materials for developing novel structures and finding ways to integrate graphene into present-day electronic devices.

Second, chemical modification of graphene's basal plane or its edges will substantially influence graphene-based devices. For electronic applications, one can imagine the

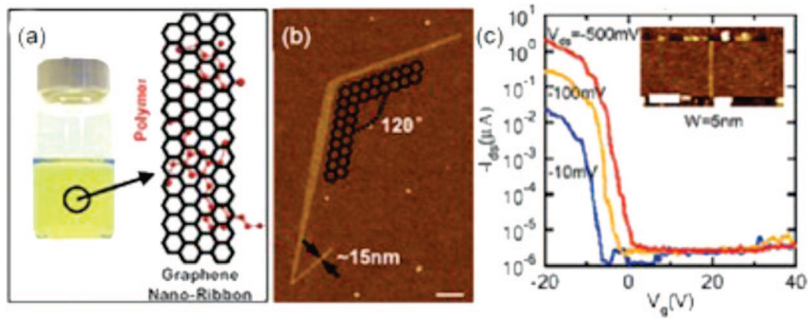

Figure 21. Solution-based method for producing graphene nanoribbons. (a) Dai's group used π-stacking polymer agents to stabilize nanoribbons in solution. (b) After spin-coating, ribbons ranging in width down to 10 nm were located by atomic force microscopy. (c) I_{on}/I_{off} ratios up to 10^6 were demonstrated. [Reprinted with permission from *Science* (http://www.aaas.org), ref 61. Copyright 2008 American Association for the Advancement of Science.]

attachment of functional groups aimed at self-assembly of simple circuits or the incorporation of chemical dopants to limit leakage current under zero gate bias. For sensors, lock-and-key type binding sites could provide selective sensitivity to a wide variety of analytes. These might include chemical warfare agents or even biological species.

Third, industrial use of graphene as a transparent conductor could have huge implications for the solar industry. As synthetic routes improve, the prospect of replacing ITO with a low-cost carbon-based coating seems feasible. This would not only remove significant uncertainty about the availability and cost of indium but also enable nonevaporative roll-to-roll processing of transparent conductors.

8. Conclusions

The field of graphene-related research has grown at a spectacular pace since single-layer flakes were first isolated in 2004. What began as an exciting material for fundamental physics has now become the focus of efforts by scientists in a wide range of disciplines. Organic and materials chemists are busily working on new synthetic routes to high-quality single layers, while engineers are designing novel devices to exploit graphene's extraordinary properties. In light of such collaborations, it is difficult to believe that the future for graphene is anything but bright.

9. Acknowledgments

The authors would like to thank the National Science Foundation's NSF-IGERT program, the UCLA-based Functional Engineering NanoArchitechtonics Focused Center Research Program (FENA-FCRP), the DARPA CERA program, and Northrop-Grumman/UC Discovery for financial support.

10. References

(1) Lu, X. K.; Yu, M. F.; Huang, H.; Ruoff, R. S. *Nanotechnology* **1999**, *10*, 269.
(2) Novoselov, K. S.; Geim, A. K.; Morozov, S. V.; Jiang, D.; Zhang, Y.; Dubonos, S. V.; Grigorieva, I. V.; Firsov, A. A. *Science* **2004**, *306*, 666.
(3) Landau, L. D. *Phys. Z. Sowjetunion* **1937**, *11*, 26.
(4) Peierls, R. E. *Ann. Inst. Henri Poincare* **1935**, *5*, 177.
(5) Stangl, J.; Holy, V.; Bauer, G. *Rev. Mod. Phys.* **2004**, *76*, 725.
(6) Meyer, J. C.; Geim, A. K.; Katsnelson, M. I.; Novoselov, K. S.; Booth, T. J.; Roth, S. *Nature* **2007**, *446*, 60.
(7) Bolotin, K. I.; Sikes, K. J.; Jiang, Z.; Klima, M.; Fudenberg, G.; Hone, J.; Kim, P.; Stormer, H. L. *Solid State Commun.* **2008**, *146*, 351.
(8) Bolotin, K. I.; Sikes, K. J.; Hone, J.; Stormer, H. L.; Kim, P. *Phys. Rev. Lett.* **2008**, *101*, 096802.
(9) Novoselov, K. S.; Jiang, D.; Schedin, F.; Booth, T. J.; Khotkevich, V. V.; Morozov, S. V.; Geim, A. K. *Proc. Natl. Acad. Sci. U.S.A.* **2005**, *102*, 10451.
(10) Geim, A. K.; Novoselov, K. S. *Nat. Mater.* **2007**, *6*, 183.
(11) Katsnelson, M. I. *Mater. Today* **2006**, *10*, 20.
(12) Novoselov, K. S.; McCann, E.; Morozov, S. V.; Fal'ko, V. I.; Katsnelson, M. I.; Zeitler, U.; Jiang, D.; Schedin, F.; Geim, A. K. *Nat. Phys.* **2006**, *2*, 177.
(13) Jiang, Z.; Zhang, Y.; Tan, Y. W.; Stormer, H. L.; Kim, P. *Solid State Commun.* **2007**, *143*, 14.
(14) Jiang, Z.; Zhang, Y.; Stormer, H. L.; Kim, P. *Phys. Rev. Lett.* **2007**, *99*, 106802.
(15) Zhang, Y. B.; Tan, Y. W.; Stormer, H. L.; Kim, P. *Nature* **2005**, *438*, 201.
(16) Novoselov, K. S.; Jiang, Z.; Zhang, Y.; Morozov, S. V.; Stormer, H. L.; Zeitler, U.; Maan, J. C.; Boebinger, G. S.; Kim, P.; Geim, A. K. *Science* **2007**, *315*, 1379.
(17) Ozyilmaz, B.; Jarillo-Herrero, P.; Efetov, D.; Abanin, D. A.; Levitov, L. S.; Kim, P. *Phys. Rev. Lett.* **2007**, *99*, 186804.
(18) Novoselov, K. S.; Geim, A. K.; Morozov, S. V.; Jiang, D.; Katsnelson, M. I.; Grigorieva, I. V.; Dubonos, S. V.; Firsov, A. A. *Nature* **2005**, *438*, 197.
(19) Morozov, S. V.; Novoselov, K. S.; Katsnelson, M. I.; Schedin, F.; Elias, D. C.; Jaszczak, J. A.; Geim, A. K. *Phys. Rev. Lett.* **2008**, *100*, 016602.
(20) Han, M.; Ozyilmaz, B.; Zhang, Y.; Jarillo-Herero, P.; Kim, P. *Phys. Status Solidi B: Basic Solid State Phys.* **2007**, *244*, 4134.
(21) Schedin, F.; Geim, A. K.; Morozov, S. V.; Hill, E. W.; Blake, P.; Katsnelson, M. I.; Novoselov, K. S. *Nat. Mater.* **2007**, *6*, 652.
(22) Novoselov, K.; Geim, A. *Mater. Technol.* **2007**, *22*, 178–179.
(23) Ruoff, R. *Nat. Nanotech.* **2008**, *3*, 10.
(24) Castro, E. V.; Novoselov, K. S.; Morozov, S. V.; Peres, N. M. R.; Dos Santos, J. M. B. L.; Nilsson, J.; Guinea, F.; Geim, A. K.; Neto, A. H. C. *Phys. Rev. Lett.* **2007**, *99*, 216802.
(25) Meyer, J. C.; Geim, A. K.; Katsnelson, M. I.; Novoselov, K. S.; Obergfell, D.; Roth, S.; Girit, C.; Zettl, A. *Solid State Commun.* **2007**, *143*, 101.
(26) Yan, J.; Henriksen, E. A.; Kim, P.; Pinczuk, A. *Phys. Rev. Lett.* **2008**, *101*, 136804.
(27) Stankovich, S.; Dikin, D. A.; Dommett, G. H. B.; Kohlhaas, K. M.; Zimney, E. J.; Stach, E. A.; Piner, R. D.; Nguyen, S. T.; Ruoff, R. S. *Nature* **2006**, *442*, 282.
(28) Stankovich, S.; Piner, R. D.; Chen, X. Q.; Wu, N. Q.; Nguyen, S. T.; Ruoff, R. S. *J. Mater. Chem.* **2006**, *16*, 155.
(29) Stankovich, S.; Dikin, D. A.; Piner, R. D.; Kohlhaas, K. A.; Kleinhammes, A.; Jia, Y.; Wu, Y.; Nguyen, S. T.; Ruoff, R. S. *Carbon* **2007**, *45*, 1558.
(30) Li, D.; Muller, M. B.; Gilje, S.; Kaner, R. B.; Wallace, G. G. *Nat. Nanotechnol.* **2008**, *3*, 101.
(31) Gilje, S.; Han, S.; Wang, M.; Wang, K. L.; Kaner, R. B. *Nano Lett.* **2007**, *7*, 3394.
(32) Hernandez, Y.; Nicolosi, V.; Lotya, M.; Blighe, F. M.; Sun, Z. Y.; De, S.; McGovern, I. T.; Holland, B.; Byrne, M.; Gun'ko, Y. K.; Boland, J. J.; Niraj, P.; Duesberg, G.; Krishnamurthy, S.; Goodhue, R.; Hutchison, J.; Scardaci, V.; Ferrari, A. C.; Coleman, J. N. *Nat. Nanotechnol.* **2008**, *3*, 563.
(33) Muller, M.; Kubel, C.; Mullen, K. *Chem.—Eur. J.* **1998**, *4*, 2099.
(34) Tyutyulkov, N.; Madjarova, G.; Dietz, F.; Mullen, K. *J. Phys. Chem. B* **1998**, *102*, 10183.
(35) Yang, X. Y.; Dou, X.; Rouhanipour, A.; Zhi, L. J.; Rader, H. J.; Mullen, K. *J. Am. Chem. Soc.* **2008**, *130*, 4216.
(36) Wu, J. S.; Pisula, W.; Mullen, K. *Chem. Rev.* **2007**, *107*, 718.
(37) Berger, C.; Song, Z. M.; Li, T. B.; Li, X. B.; Ogbazghi, A. Y.; Feng, R.; Dai, Z. T.; Marchenkov, A. N.; Conrad, E. H.; First, P. N.; de Heer, W. A. *J. Phys. Chem. B* **2004**, *108*, 19912.
(38) Berger, C.; Song, Z. M.; Li, X. B.; Wu, X. S.; Brown, N.; Naud, C.; Mayou, D.; Li, T. B.; Hass, J.; Marchenkov, A. N.; Conrad, E. H.; First, P. N.; de Heer, W. A. *Science* **2006**, *312*, 1191.
(39) de Heer, W. A.; Berger, C.; Wu, X. S.; First, P. N.; Conrad, E. H.; Li, X. B.; Li, T. B.; Sprinkle, M.; Hass, J.; Sadowski, M. L.; Potemski, M.; Martinez, G. *Solid State Commun.* **2007**, *143*, 92.
(40) Hass, J.; de Heer, W. A.; Conrad, E. H. *J. Phys.: Condens. Matter* **2008**, *20*, 323202.
(41) Reina, A.; Jia, X. T.; Ho, J.; Nezich, D.; Son, H. B.; Bulovic, V.; Dresselhaus, M. S.; Kong, J. *Nano Lett.* **2009**, *9*, 30.
(42) Kim, K. S. *Nature* **2009**, *457*, 706.
(43) Sutter, P. W.; Flege, J. I.; Sutter, E. A. *Nat. Mater.* **2008**, *7*, 406.
(44) Gomez-Navarro, C.; Weitz, R. T.; Bittner, A. M.; Scolari, M.; Mews, A.; Burghard, M.; Kern, K. *Nano Lett.* **2007**, *7*, 3499.
(45) Kam, N. W. S.; Liu, Z.; Dai, H. J. *J. Am. Chem. Soc.* **2005**, *127*, 12492.
(46) Shim, M.; Kam, N. W. S.; Chen, R. J.; Li, Y. M.; Dai, H. J. *Nano Lett.* **2002**, *2*, 285.
(47) Strano, M. S.; Dyke, C. A.; Usrey, M. L.; Barone, P. W.; Allen, M. J.; Shan, H. W.; Kittrell, C.; Hauge, R. H.; Tour, J. M.; Smalley, R. E. *Science* **2003**, *301*, 1519.
(48) Boul, P. J.; Liu, J.; Mickelson, E. T.; Huffman, C. B.; Ericson, L. M.; Chiang, I. W.; Smith, K. A.; Colbert, D. T.; Hauge, R. H.; Margrave, J. L.; Smalley, R. E. *Chem. Phys. Lett.* **1999**, *310*, 367.
(49) Holzinger, M.; Vostrowsky, O.; Hirsch, A.; Hennrich, F.; Kappes, M.; Weiss, R.; Jellen, F. *Angew. Chem., Int. Ed.* **2001**, *40*, 4002.
(50) Georgakilas, V.; Kordatos, K.; Prato, M.; Guldi, D. M.; Holzinger, M.; Hirsch, A. *J. Am. Chem. Soc.* **2002**, *124*, 760.
(51) Das Sarma, S.; Geim, A. K.; Kim, P.; MacDonald, A. H. *Solid State Commun.* **2007**, *143*, 1.
(52) Neto, A. H. C.; Guinea, F.; Peres, N. M. R.; Novoselov, K. S.; Geim, A. K. *Rev. Mod. Phys.* **2009**, *81*, 109.
(53) *Graphite intercalation compounds and applications*; Endo, M., Ed.; Oxford University Press: 2003.
(54) Delhaes, P. *Graphite and precursors*; CRC Press: 2001.
(55) Survey, U. S. G., 2007.

(56) Toshiaki Enoki, M. S.; Morinobu Endo. *Graphite intercalation compounds and applications*; Oxford University Press: 2003.
(57) Shaffault, P. J. *J. Prakt. Chem.* **1841**, *21*, 155.
(58) Dresselhaus, M. S.; Dresselhaus, G. *Adv. Phys.* **2002**, *51*, 186.
(59) Viculis, L. M.; Mack, J. J.; Kaner, R. B. *Science* **2003**, *299*, 1361.
(60) Viculis, L. M.; Mack, J. J.; Mayer, O. M.; Hahn, H. T.; Kaner, R. B. *J. Mater. Chem.* **2005**, *15*, 974.
(61) Li, X. L.; Wang, X. R.; Zhang, L.; Lee, S. W.; Dai, H. J. *Science* **2008**, *319*, 1229.
(62) Kouvetakis, J.; Kaner, R. B.; Sattler, M. L.; Bartlett, N. *J. Chem. Soc.—Chem. Commun.* **1986**, 1758.
(63) Kaner, R. B.; Kouvetakis, J.; Warble, C. E.; Sattler, M. L.; Bartlett, N. *Mater. Res. Bull.* **1987**, *22*, 399.
(64) Jiang, D. E.; Sumpter, B. G.; Dai, S. *J. Chem. Phys.* **2007**, *126*, 134701–134701-6.
(65) Miyata, Y.; Kawai, T.; Miyamoto, Y.; Yanagi, K.; Maniwa, Y.; Kataura, H. *J. Phys. Chem. C* **2007**, *111*, 9671.
(66) Kawai, T.; Miyamoto, Y. *Chem. Phys. Lett.* **2008**, *453*, 256.
(67) Girit, C. O.; Meyer, J. C.; Erni, R.; Rossell, M. D.; Kisielowski, C.; Yang, L.; Park, C.-H.; Crommie, M. F.; Cohen, M. L.; Louie, S. G.; Zettl, A. *Science* **2009**, *323*, 1705.
(68) Zhang, Y. B.; Small, J. P.; Pontius, W. V.; Kim, P. *Appl. Phys. Lett.* **2005**, *86*, 073104-1.
(69) Affoune, A. M.; Prasad, B. L. V.; Sato, H.; Enoki, T.; Kaburagi, Y.; Hishiyama, Y. *Chem. Phys. Lett.* **2001**, *348*, 17.
(70) Nair, R. R.; Blake, P.; Grigorenko, A. N.; Novoselov, K. S.; Booth, T. J.; Stauber, T.; Peres, N. M. R.; Geim, A. K. *Science* **2008**, *320*, 1308.
(71) Stauber, T.; Peres, N. M. R.; Geim, A. K. *Phys. Rev. B* **2008**, *78*, 085432.
(72) Blake, P.; Hill, E. W.; Neto, A. H. C.; Novoselov, K. S.; Jiang, D.; Yang, R.; Booth, T. J.; Geim, A. K. *Appl. Phys. Lett.* **2007**, *91*, 063124.
(73) Blake, P.; Brimicombe, P. D.; Nair, R. R.; Booth, T. J.; Jiang, D.; Schedin, F.; Ponomarenko, L. A.; Morozov, S. V.; Gleeson, H. F.; Hill, E. W.; Geim, A. K.; Novoselov, K. S. *Nano Lett.* **2008**, *8*, 1704.
(74) Jung, I.; Pelton, M.; Piner, R.; Dikin, D. A.; Stankovich, S.; Watcharotone, S.; Hausner, M.; Ruoff, R. S. *Nano Lett.* **2007**, *7*, 3569.
(75) Ni, Z. H.; Chen, W.; Fan, X. F.; Kuo, J. L.; Yu, T.; Wee, A. T. S.; Shen, Z. X. *Phys. Rev. B* **2008**, *77*, 115416.
(76) Batra, I. P.; Garcia, N.; Rohrer, H.; Salemink, H.; Stoll, E.; Ciraci, S. *Surf. Sci.* **1987**, *181*, 126.
(77) Rabe, J. P.; Buchholz, S. *Science* **1991**, *253*, 424.
(78) Soler, J. M.; Baro, A. M.; Garcia, N.; Rohrer, H. *Phys. Rev. Lett.* **1986**, *57*, 444.
(79) Stolyarova, E.; Rim, K. T.; Ryu, S. M.; Maultzsch, J.; Kim, P.; Brus, L. E.; Heinz, T. F.; Hybertsen, M. S.; Flynn, G. W. *Proc. Natl. Acad. Sci. U.S.A.* **2007**, *104*, 9209.
(80) Ferrari, A. C.; Meyer, J. C.; Scardaci, V.; Casiraghi, C.; Lazzeri, M.; Mauri, F.; Piscanec, S.; Jiang, D.; Novoselov, K. S.; Roth, S.; Geim, A. K. *Phys. Rev. Lett.* **2006**, *97*, 187401.
(81) Ferrari, A. C.; Robertson, J. *Phys. Rev. B* **2000**, *61*, 14095.
(82) Casiraghi, C.; Pisana, S.; Novoselov, K. S.; Geim, A. K.; Ferrari, A. C. *Appl. Phys. Lett.* **2007**, *91*, 233108.
(83) Ferrari, A. C. *Solid State Commun.* **2007**, *143*, 47.
(84) Calizo, I.; Balandin, A. A.; Bao, W.; Miao, F.; Lau, C. N. *Nano Lett.* **2007**, *7*, 2645.
(85) Matthews, M. J.; Pimenta, M. A.; Dresselhaus, G.; Dresselhaus, M. S.; Endo, M. *Phys. Rev. B* **1999**, *59*, R6585.
(86) Gupta, A.; Chen, G.; Joshi, P.; Tadigadapa, S.; Eklund, P. C. *Nano Lett.* **2006**, *6*, 2667.
(87) Wallace, P. R. *Phys. Rev.* **1947**, *71*, 476.
(88) Slonczewski, J. C.; Weiss, P. R. *Phys. Rev.* **1958**, *109*, 272.
(89) Hwang, E. H.; Adam, S.; Das Sarma, S. *Phys. Rev. Lett.* **2007**, *98*, 186806.
(90) Novoselov, K. S.; Morozov, S. V.; Mohinddin, T. M. G.; Ponomarenko, L. A.; Elias, D. C.; Yang, R.; Barbolina, I. I.; Blake, P.; Booth, T. J.; Jiang, D.; Giesbers, J.; Hill, E. W.; Geim, A. K. *Phys. Status Solidi B: Basic Solid State Phys.* **2007**, *244*, 4106.
(91) Morozov, S. V.; Novoselov, K. S.; Geim, A. K. *Phys.—Usp.* **2008**, *51*, 744.
(92) Alivisatos, P. *Nat. Biotechnol.* **2004**, *22*, 47.
(93) Chen, R. J.; Bangsaruntip, S.; Drouvalakis, K. A.; Kam, N. W.; Shim, M.; Li, Y.; Kim, W.; Utz, P. J.; Dai, H. *Proc. Natl. Acad. Sci. U. S. A.* **2003**, *100*, 4984.
(94) Chen, R. J.; Zhang, Y.; Wang, D.; Dai, H. *J. Am. Chem. Soc.* **2001**, *123*, 3838.
(95) Wang, J. *Electroanalysis* **2005**, *17*, 7.
(96) Jung, I.; Dikin, D. A.; Piner, R. D.; Ruoff, R. S. *Nano Lett.* **2008**, *8*, 4283.
(97) Yang, D.; Velamakanni, A.; Bozoklu, G.; Park, S.; Stoller, M.; Piner, R. D.; Stankovich, S.; Jung, I.; Field, D. A.; Ventrice, C. A.; Ruoff, R. S. *Carbon* **2009**, *47*, 145.
(98) Jeong, H.-K.; Lee, Y. P.; Lahaye, R. J. W. E.; Park, M.-H.; An, K. H.; Kim, I. J.; Yang, C.-W.; Park, C. Y.; Ruoff, R. S.; Lee, Y. H. *J. Am. Chem. Soc.* **2008**, *130*, 1362.
(99) Hummers, W. S.; Offeman, R. E. *J. Am. Chem. Soc.* **1958**, *80*, 1339.
(100) Watcharotone, S.; Dikin, D. A.; Stankovich, S.; Piner, R.; Jung, I.; Dommett, G. H. B.; Evmenenko, G.; Wu, S. E.; Chen, S. F.; Liu, C. P.; Nguyen, S. T.; Ruoff, R. S. *Nano Lett.* **2007**, *7*, 1888.
(101) Tung, V. C.; Allen, M. J.; Yang, Y.; Kaner, R. B. *Nat. Nanotechnol.* **2009**, *4*, 25.
(102) Allen, M. J.; Fowler, J. D.; Tung, V. C.; Yang, Y.; Weiller, B. H.; Kaner, R. B. *Appl. Phys. Lett.* **2008**, *93*, 193119.
(103) Fowler, J. D.; Allen, M. J.; Tung, V. C.; Yang, Y.; Kaner, R. B.; Weiller, B. H. *ACS Nano* **2009**, *3*, 301.
(104) Schmidt, E. W. *Hydrazine and its derivatives*; Wiley-Interscience: New York, 2001.
(105) Dikin, D. A.; Stankovich, S.; Zimney, E. J.; Piner, R. D.; Dommett, G. H. B.; Evmenenko, G.; Nguyen, S. T.; Ruoff, R. S. *Nature* **2007**, *448*, 457.
(106) Park, S.; Lee, K. S.; Bozoklu, G.; Cai, W.; Nguyen, S. T.; Ruoff, R. S. *ACS Nano* **2008**, *2*, 572.
(107) Cote, L. J.; Kim, F.; Huang, J. *J. Am. Chem. Soc.* **2009**, *131*, 1043.
(108) Wu, J. H.; Tang, Q. W.; Sun, H.; Lin, J. M.; Ao, H. Y.; Huang, M. L.; Huang, Y. F. *Langmuir* **2008**, *24*, 4800.
(109) Li, X.; Zhang, G.; Bai, X.; Sun, X.; Wang, X.; Wang, E.; Dai, H. *Nat. Nanotechnol.* **2008**, *3*, 538.
(110) Robinson, J. T.; Perkins, F. K.; Snow, E. S.; Wei, Z. Q.; Sheehan, P. E. *Nano Lett.* **2008**, *8*, 3137.
(111) Wang, X.; Zhi, L. J.; Mullen, K. *Nano Lett.* **2008**, *8*, 323.
(112) Eda, G.; Fanchini, G.; Chhowalla, M. *Nat. Nanotechnol.* **2008**, *3*, 270.
(113) Eda, G.; Lin, Y. Y.; Miller, S.; Chen, C. W.; Su, W. F.; Chhowalla, M. *Appl. Phys. Lett.* **2008**, *92*, 233305.
(114) Berresheim, A. J.; Muller, M.; Mullen, K. *Chem. Rev.* **1999**, *99*, 1747–1785.
(115) Dotz, F.; Brand, J. D.; Ito, S.; Gherghel, L.; Mullen, K. *J. Am. Chem. Soc.* **2000**, *122*, 7707.
(116) Watson, M. D.; Fechtenkotter, A.; Mullen, K. *Chem. Rev.* **2001**, *101*, 1267–1300.
(117) Gutman, I.; Tomovic, Z.; Mullen, K.; Rabe, E. P. *Chem. Phys. Lett.* **2004**, *397*, 412.
(118) Kedzierski, J.; Hsu, P. L.; Healey, P.; Wyatt, P. W.; Keast, C. L.; Sprinkle, M.; Berger, C.; de Heer, W. A. *IEEE Trans. Electron Devices* **2008**, *55*, 2078.
(119) Berger, C.; Song, Z. M.; Li, X. B.; Wu, X. S.; Brown, N.; Maud, D.; Naud, C.; de Heer, W. A. *Phys. Status Solidi A: Appl. Mater. Sci.* **2007**, *204*, 1746.
(120) Sadowski, M. L. E. A. *J. Phys. Chem. Solids* **2006**, *67*, 2172.
(121) Brar, V. W.; Zhang, Y.; Yayon, Y.; Ohta, T.; McChesney, J. L.; Bostwick, A.; Rotenberg, E.; Horn, K.; Crommie, M. F. *Appl. Phys. Lett.* **2007**, *91*, 122102.
(122) Rotenberg, E.; Bostwick, A.; Ohta, T.; McChesney, J. L.; Seyller, T.; Horn, K. *Nat. Mater.* **2008**, *7*, 258.
(123) Ozyilmaz, B.; Jarillo-Herrero, P.; Efetov, D.; Kim, P. *Appl. Phys. Lett.* **2007**, *91*, 192107.
(124) Han, M. Y.; Ozyilmaz, B.; Zhang, Y. B.; Kim, P. *Phys. Rev. Lett.* **2007**, *98*, 206805.
(125) Li, D.; Kaner, R. B. *Science* **2008**, *320*, 1170.

CR900070D